Wind-Stress Coefficients over Sea Surface near Neutral Conditions—A Revisit

JIN WU

College of Marine Studies, University of Delaware, Newark 19711

(Manuscript received 18 June 1979, in final form 7 January 1980)

ABSTRACT

A scaling law of wind-stress coefficients is presented to illustrate explicitly that the coefficient increases with wind velocity and decreases with fetch; physical reasonings of both trends are discussed. Besides being shown previously to be related to a criterion determining airflow separation from waves, the Charnock relation is further associated with the critical roughness Reynolds number identifying regimes of the atmospheric surface layer. Intrinsic errors and limitations of the Charnock relation, which provides an overall correlation between stress coefficient and wind velocity, are illustrated. A probable nondimensional expression, a refinement of the Charnock relation, is proposed between the roughness length and the wind-friction velocity involving not only gravity but also surface tension and viscosity. Previous compilation of wind-stress data obtained with eddy-correlation and wind-profile methods is found to be consistent with recent results obtained with similar techniques. A single, linear law empirical formula for estimating oceanic wind-stress coefficients at all wind velocities is suggested, and appears to provide a better representation than the power law formula proposed earlier. Finally, recent results on relating roughness length to sea surface irregularities and on relating stress coefficient to roughness Reynolds number and to dominant wave characteristics are discussed.

1. Introduction

Studies of wind-wave interaction in the last decade evolved around the Charnock (1955) relation with roughness length describing the wind-disturbed water surface as being proportional to the ratio between the square of wind-friction velocity and gravitational acceleration. The values of the proportionality constant, however, are scattered, and the physical basis for the application of the Charnock relation in the field is not so clear as that in the laboratory. It appears that although the Charnock relation provides an overall correlation of the stress coefficient with wind velocity and fetch, the time may be ripe to reexamine this relationship.

Recent studies of the wind-stress coefficient over the sea surface have concentrated on variations (or constancy) of the stress coefficient with wind velocity. On the basis of a logarithmic wind velocity profile and the Charnock relation, a Froude-number scaling law of wind-stress coefficients has been derived and confirmed by laboratory and oceanic data (Wu, 1969a,b). According to this scaling law, the wind-stress coefficient should increase with wind velocity and decrease with fetch. Nonetheless, despite general acceptance of the logarithmic wind profile and the Charnock relation, the argument for dependency of stress coefficient on wind velocity still goes on, with little attention paid on its dependency on fetch. Recent reviews by Smith and Banke (1975) and Garratt (1977), however, confirm essentially the same variation of stress coefficient with wind velocity as reported earlier by Wu (1969a). The time also may be ripe to see whether recent refinement of measurement and analysis has indeed produced results differing from earlier data.

In this study, the data compiled earlier (Wu, 1969a) are selected and supplemented by recent results to provide a better understanding and a more accurate estimation of the wind stress. The variations of stress coefficient with wind velocity and with fetch are explicitly derived, and attempts were made to explain physically both trends and to clarify the discontinuity of the wind-stress coefficient at low and high wind velocities. Earlier proposals on flow separation related to wave breaking (Wu, 1968, 1969c) and on ripples acting as roughness elements (Wu, 1970) are also further explored on the basis of comprehensive data compiled herewith and of recent studies on airflow separation (Wu, 1970; Banner and Melville, 1976; Melville, 1977). A probable, refined, nondimensional relationship describing the equilibrium state of wind-wave interaction, incorporating the effects of surface tension and viscosity with those of gravity, is presented. We have also discussed recent proposals for relating the roughness length to sea surface irregularities (Kondo *et al.*, 1973), and for relating the wind-stress coefficient to characteristics of dominant waves (Hsu, 1974) and to the roughness Reynolds number (Sethu-

0022-3670/80/050727-14$07.50

Raman and Raynor, 1975). Finally, the earlier data (Wu, 1969a) excluding those obtained with the surface tilting method are shown in close agreement with recent results, indicating that we may already have a rather reliable determination of the wind stress over the sea surface. More studies, however, are suggested for very high wind velocities (hurricanes) and for uncovering new parameters influencing wind-wave interactions.

2. Fundamentals on wind-wave interaction developed from Charnock relation

Recent discussions of wind-stress coefficients and, consequently, of roughness lengths, have concentrated on the Charnock relation. In this section, previous results are summarized and further explored.

a. Logarithmic wind profile, Charnock relation, and wind and fetch dependency of stress coefficients

1) General

Earlier as well as recent measurements have confirmed the logarithmic nature of the wind profile near, but not overly close, to the water surface (Roll, 1965), i.e.,

$$\frac{U_z}{u_*} = \frac{1}{\kappa} \ln\left(\frac{z}{z_0}\right), \tag{1}$$

where U_z is the wind velocity at a height z above mean sea level; u_* is the friction velocity of the wind, $u_* = (\tau/\rho)^{1/2}$, in which τ is the wind stress and ρ the density of air; κ is the von Kármán constant; and z_0 is the roughness length of the sea surface.

An empirical formula was suggested on dimensional grounds by Charnock (1955):

$$\frac{z_0}{u_*^2/g} = \text{constant} = a, \tag{2}$$

in which g is the gravitational acceleration, and a is the so-called Charnock constant. Subsequently, this expression was rationalized by Wu (1968) as an equation of state characterizing equilibrium interaction between the wind and waves with gravity waves acting as roughness elements. More on the relevance and limitation of the Charnock relation will be discussed in a later section. It suffices for now to say that the existence of the Charnock relation has been supported earlier, among others by Kitaigorodskii and Volkov (1965) and Roll (1965), and recently by a great majority of investigators (Garratt, 1977).

Substituting Eq. (2) into Eq. (1) yields an expression for determining the stress coefficients at various fetches under different wind velocities (Wu, 1969b):

$$C_z = \frac{\tau}{\rho U_z^2} = \left(\frac{u_*}{U_z}\right)^2 = \left[\frac{\kappa}{\ln(1/aC_zF^2)}\right]^2, \quad F = \frac{U_z}{(gZ)^{1/2}}, \tag{3}$$

wherein C_z is the wind-stress coefficient, Z the anemometer height located within the constant flux layer (for clarity, z instead of Z is still used for the subscript), and F is the Froude number. For oceanic conditions with the standard anemometer height of 10 m, we have $F \approx U_{10}/10$, where U_{10} is in meters per second measured at the standard anemometer height. The correlation shown in Eq. (3) has been verified earlier (Wu, 1969b) with laboratory and oceanic data obtained at extremely different fetches, and is shown with presently compiled data in Fig. 1. The value of $a = 0.0156$ was chosen (Wu, 1969b) to provide the best correlation between laboratory and oceanic results. The laboratory data at two lowest wind velocities, where surface tension rather than gravity governs wind-wave interaction (Wu, 1968), are omitted for Fig. 1. The suggested anemometer heights for various fetches and wind velocities (Wu, 1971) are shown in the insert of Fig. 1; the values are

$$\left.\begin{aligned} &Z = 10 \text{ cm}, && R < 5 \times 10^7 \\ &Z = 7.35 \times 10^{-5}\, R \text{ (cm)}, && 5 \times 10^7 < R < 5 \times 10^{10} \\ &Z = 10 \text{ m}, && R > 5 \times 10^{10} \end{aligned}\right\} \tag{4}$$

where L is the fetch, ν the kinematic viscosity of air, and $R = U_z L/\nu$ is the fetch Reynolds number. The nondimensional plot shown in Fig. 1 represents the first, and still is the only, nondimensional presentation[1] of the wind-stress coefficient.

As will be discussed in a later section, the values of the Charnock constant (a) suggested by various investigators generally fall within the range of 0.012 and 0.035. For various values of a, the wind-stress coefficients were calculated from Eqs. (3) and (4) and are shown in Fig. 2 under various wind velocities with $Z = 10$ m, and at different fetches with $U_Z = 10$ m s^{-1}. A rather strong dependency of the stress coefficient on wind velocity is shown for oceanic fetches with $Z = 10$ m. Notice, however, that according to Eq. (4) $Z = 10$ m for $L > 75$ km; therefore, the fetch dependency of the stress coefficient shown in Fig. 2 includes the effect of a variable reference height for $L < 75$ km. It is also shown in the figure that the increase of the coefficient with

[1] As emphasized by Hasselmann (Favre and Hasselmann, 1978, p. 50), the wind-stress coefficient, a dimensionless parameter, should be plotted against another dimensionless parameter instead of wind velocity.

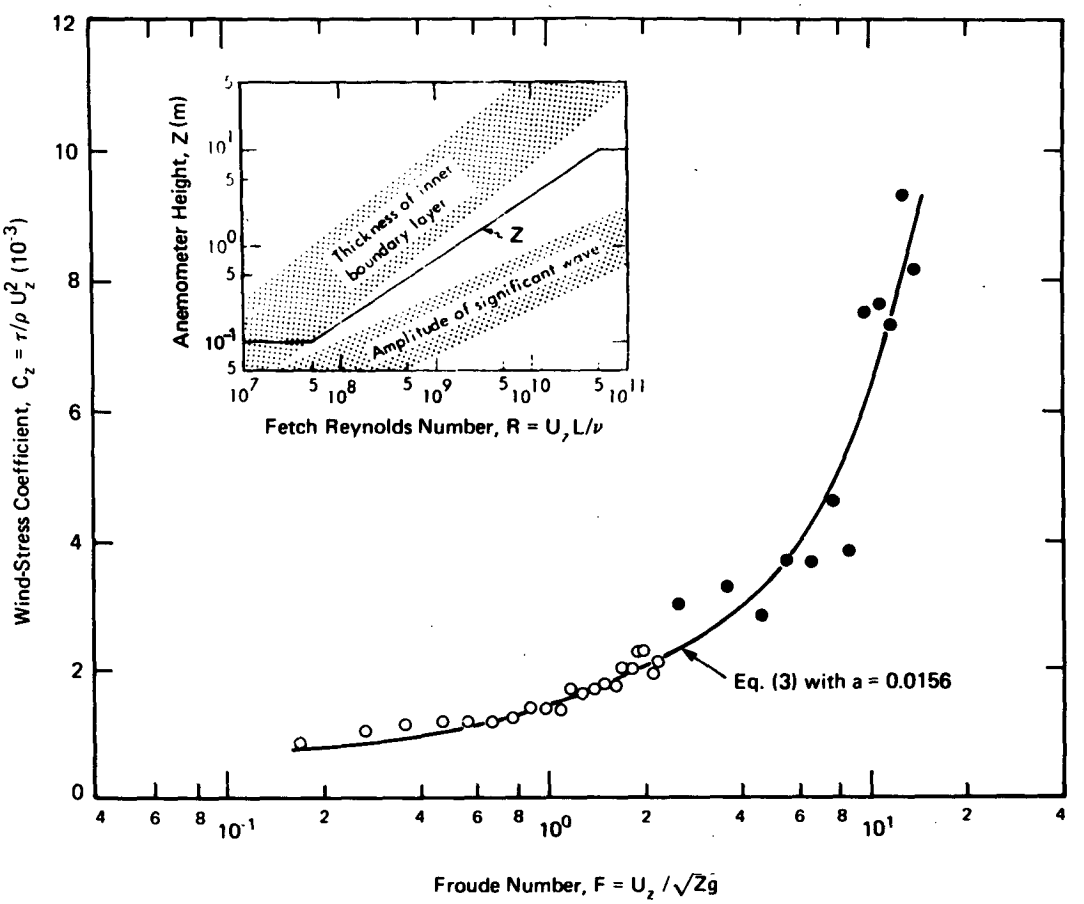

FIG. 1. Froude number scaling of wind-stress coefficients. The open circles are oceanic data with Z = 10 m, the solid circles are laboratory data with Z = 10 cm, and the anemometer heights for intermediate fetches are shown in the insert.

wind velocity is only nearly linear, and the rate of increase is smaller at a higher wind velocity. The dependency of the stress coefficient on fetch is rather weak at long fetches. For both variations of C_{10} with U_{10} and of C_{10} with L, the dependency is stronger for a greater value of a. Not shown here are the variations of C_{10} with fetch under various wind velocities, where the variation is greater at a higher wind velocity.

The results in Fig. 2 show explicitly that the stress coefficient determined in laboratory tanks with short fetches is much greater than that determined in the field with long fetches. Such a trend, also illustrated by the data in Fig. 1, definitely indicates that the laboratory and field results on wind-driven phenomena, including wind stress, should not be compared on the basis of wind velocity, as is customarily done.

2) OCEANIC CASE

The general expression of the wind-stress coefficient under different wind velocities at various fetches is shown in Eq. (3), with the anemometer height determined from Eq. (4). These two equations encompass the growth of roughness length and the development of the airflow boundary layer with wind velocity and fetch. For the oceanic case, the development of the atmospheric surface layer becomes gradual, the anemometer height as discussed earlier being kept at 10 m. From Eq. (1), the wind-stress coefficient in this case can be shown to be related entirely to the roughness length (Roll, 1965) i.e.,

$$C_{10} = \frac{\tau}{\rho U_{10}^2} = \frac{\kappa}{\ln(Z/z_0)}, \quad Z = 10 \text{ m}. \qquad (5)$$

It should be emphasized that for the same wind *condition* the reference velocity (U_{10}) in this case varies longitudinally. This is unlike flows in pipes where the cross-sectional average velocity is used, or for flows over a flat plate where the free-stream velocity is used. Because of the variation of the reference wind velocity in Eq. (5), the Charnock relation is still indispensable in determining the variation of the roughness length with wind velocity.

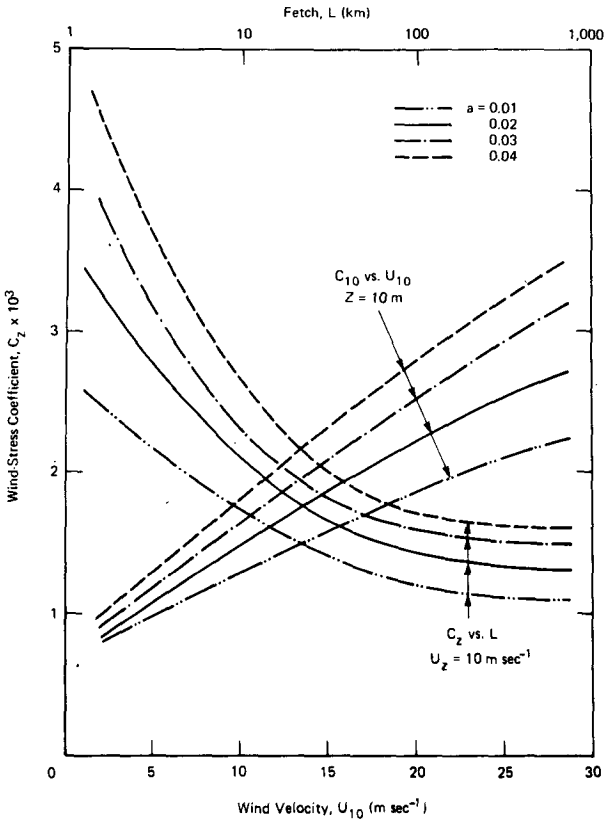

FIG. 2. Variations of wind-stress coefficients with Charnock constant, wind velocity and fetch.

The roughness elements, as discussed later, consist of short waves, which for a given wind condition have reached a saturated state at most oceanic fetches and varied insignificantly thereafter. Consequently, the wind-stress coefficients at upwind and downwind fetches are the same according to Eq. (5) for a given wind condition with the same roughness length. However, for the same wind condition, the wind velocity at the downwind fetch is slightly smaller than that at the upwind fetch due to the thickening of the surface layer. Taking together the equality of the wind-stress coefficients and the inequality of the wind velocity, the wind stress at the upwind fetch should be greater than that at the downwind fetch. In summary, for the same wind condition at oceanic fetches, where the spatial rate of wave growth becomes gradual with wave drag becoming secondary in comparison with the wind stress, we have

$$z_{0_u} = z_{0_d}, \quad C_{10_u} = C_{10_d}, \quad \text{where}$$
$$U_{10_u} > U_{10_d}, \quad \tau_u > \tau_d, \tag{6}$$

where the subscript u indicates an upwind fetch and d a downwind fetch. Following Eq. (6), for the same wind condition, we have again

$$C_{10_u} = \frac{\tau_u}{\rho U_{10_u}{}^2} = \frac{\tau_d}{\rho U_{10_d}{}^2} = \frac{\tau_d}{\rho(U_{10_u} - \Delta U)^2} = C_{10_d}, \tag{7}$$

in which $\Delta U = U_{10_u} - U_{10_d}$ is the wind-velocity differential and is always positive.

On the other hand, for the same wind *velocity* to make the wind velocity at the downwind fetch equal to that at the upwind fetch, we can illustrate through the following sequence that the wind-stress coefficient at a longer fetch is smaller:

$$C_{10_u} = \frac{\tau_u}{\rho U_{10}{}^2} = \frac{\tau_d}{\rho(U_{10} - \Delta U)^2} = \frac{\tau_d}{\rho U_{10}{}^2} \times \frac{U_{10}{}^2}{(U_{10} - \Delta U)^2} > \frac{\tau_d}{\rho U_{10}{}^2} = C_{10_d}, \tag{8}$$

where the subscripts on U_{10} have been dropped in favor of the equality shown in Eq. (6). Admittedly, the velocity differential is small, but the correction is amplified through the square of the velocity ratio $U_{10}{}^2/(U_{10} - \Delta U)^2$.

In summary, even though the oceanic case exhibits a unique relationship between the wind-stress coefficient and roughness length, the Charnock relation is still needed to describe the growth of roughness length with wind velocity. For the long fetches discussed in this section, the roughness length for the same wind condition no longer increases with the fetch, and the wind-stress coefficient for the same wind velocity should decrease, although very weakly, with fetch as shown in Fig. 2. For short fetches, the variation of direct momentum input to waves may account for most of the fetch dependency of the stress coefficient.

b. Airflow-separation criterion, the Charnock relation and roughness length

On the basis of experimental evidence, a criterion for determining airflow separation from wind waves was proposed by Wu (1969c): *airflow separation occurs from waves having a phase velocity less than the wind-friction velocity*. Recent experimental studies (Banner and Melville, 1976), numerical calculations (Gent and Taylor, 1977) and data analysis (Melville, 1977) all tend to support this criterion. The waves from which the airflow separates are the roughness elements, and the height of these waves should therefore correspond to the roughness length.

The Charnock relation discussed in the preceding section was suggested on dimensional grounds, while the separation criterion was established on physical evidence. Both efforts nevertheless involve the same group of physical parameters, and were cor-

related subsequently by Wu (1970) with $a = 0.027$. The following sequence illustrates this correlation:

$$u_* = (gz_0/a)^{1/2} = [g(k/30)/0.027]^{1/2} = [g(\lambda/7)/0.81]^{1/2} \approx (g\lambda/2\pi)^{1/2} \approx c, \quad (9)$$

wherein the height of roughness elements k is considered to be 30 times the roughness length, i.e., $k = 30z_0$ (Schlichting, 1968); the wave from which the airflow separates has the maximum wave steepness $k/\lambda = 1/7$ (λ is the wavelength) (Roll, 1965); and the phase velocity of waves follows the dispersion relationship $c = (g\lambda/2\pi)^{1/2}$. It should be emphasized that the gravitational acceleration is considered an essential dynamic parameter in the Charnock relation rather than merely an added constant, as indicated by Garratt (1977).

The scattered values of the Charnock constant have a rather small influence on the general derivation of Eq. (9), in which the square root of a is involved. If the value of the Charnock constant 0.0185 determined in a later section is used, we have $u_* \approx 6c/5$. The separation criterion was first derived from results of wind-wave interaction obtained by Wu (1969c) in a laboratory tank, where the roughness length, and consequently the length of surface waves acting as roughness elements, is actually much greater than that in the field. Inasmuch as the effects of wind-induced drift currents on the propagation of surface waves are greater for shorter waves, the propagation of waves acting as roughness elements in laboratory tanks is, therefore, insignificantly modified while that in the field is greatly influenced. The observed phase velocity of waves acting as roughness elements in the field can be in excess of that calculated from the dispersion relation by as much as the wind-induced sea surface drift current, or about $u_*/2$ (Wu, 1975). Therefore, it is not surprising to see that the wind-friction velocity in the field should be slightly greater than the calculated phase velocity of waves (roughness elements) from which the airflow separates. The explanation for the use of the dispersion relationship for gravity waves is that, as shown below, the wavelength of roughness elements ($7k$) is generally greater than 1.73 cm, with gravitational rather than surface tension effects being more important.

From the compiled and averaged wind-stress coefficients presented in a later section, the height of the roughness elements (k) can be calculated from z_0 obtained from Eq. (5) without the Charnock relation, and can also be predicted from the Charnock relation shown in Eq. (9). The height obtained from Eq. (5) with the wind-stress coefficients shown in later sections is designated as k_g, and the height obtained from Eq. (9) according to the criterion for determining airflow separation from roughness elements, with $a = 0.0185$, is designated as k_p. These two quantities calculated at every integral wind velocity are plotted against each other in Fig. 3. An excellent correlation is seen except for few points ($U_{10} < 5$ m s^{-1}) where the atmospheric surface layer is aerodynamically smooth. This close correlation further substantiates the separation criterion.

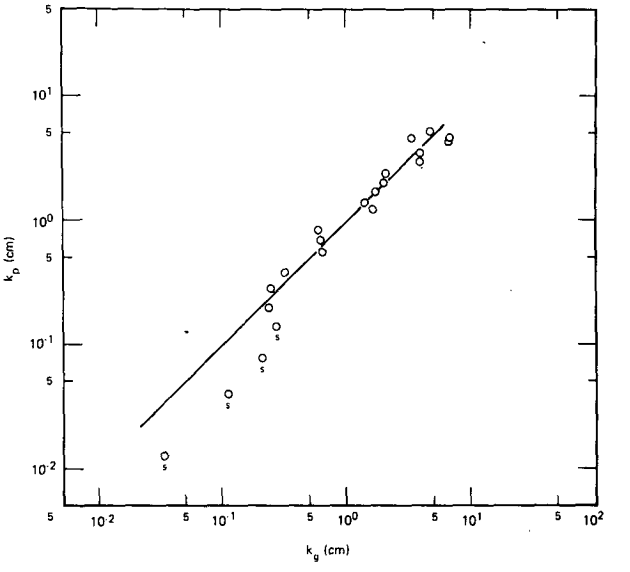

FIG. 3. Heights of roughness elements predicted by separation criterion (k_p) and calculated from wind-stress coefficient (k_g). The data points marked with s appear to be with the atmospheric surface layer in the aerodynamically smooth flow regime.

3. Oceanic wind-stress data and analysis

It is known that the wind-stress coefficient is influenced by the stability of the atmospheric surface layer. Stability conditions were not specifically reported in many earlier investigations, most of which, however, are believed to have been conducted under nearly neutral conditions. Recent measurements obtained under reportedly nearly neutral conditions are examined in this section. Furthermore, the earlier averaging of all data compiled from various sources (Wu, 1969a) prevented examination of the trend of each individual set. Such a procedure was imposed by the limited extent of the data in most of earlier investigations. The data published in recent works are more extensive; it is now possible to examine each set separately.

The previous compilation (Wu, 1969a) consists of data from 12 laboratory investigations and 30 field studies; from the latter, 21 studies are retained, and another 12 sets of recent independent field investigations are added to the present compilation.

TABLE 1. Dependence of stress coefficient on wind velocity.

Investigator	Range of wind velocity (m s^{-1})	n ($u_* \approx U_{10}^n$)	$m = 2(n-1)$ ($C_{10} \approx U_{10}^m$)
Brocks and Krugermeyer (1970)	4.1–13	1.04	0.08
Miyake *et al.* (1970)	4–9	1.13	0.26
Hicks and Dyer (1970)	2–9.4	1.14	0.28
De Leonibus (1971)	4.5–14	1.17	0.34
Pond *et al.* (1971)	4–8	1.13	0.26
Hicks (1972)	3.1–9.7	1.15	0.30
Kondo *et al.* (1972)	1.9–20.3	1.28	0.56
Sheppard *et al.* (1972)	2.3–16.2	1.37	0.74
Demman and Miyake (1973)	4.4–17.5	1.05	0.10
Smith (1974)	3.1–10.2	1.18	0.36
Wieringa (1974)	4.5–15	1.20	0.40
Smith and Banke (1975)	2.5–21	1.33	0.66

a. Wind-velocity dependency of stress coefficients

1) SOME RECENT MEASUREMENTS

The following power law was suggested (Wu, 1969a) as the simplest possible form to approximate the wind-stress coefficient for the open sea:

$$C_{10} = 0.5 U_{10}^{1/2} \times 10^{-3}, \tag{10}$$

in which U_{10} is expressed in meters per second. As discussed earlier, the above equation is dimensionally inhomogeneous; however, it is convenient for practical applications. The most recent review by Garratt (1977) suggested essentially the same law: $C_{10} = 0.51 U_{10}^{0.46} \times 10^{-3}$. In order to explore further such a power-law relationship between the wind-stress coefficient and wind velocity, recent data obtained in various investigations were compiled and replotted on logarithmic scales with wind-friction velocity, instead of the wind-stress coefficient, versus the wind velocity. It was found that a straight line could indeed fit very closely to each set of data, and the slope n of the fitted line, $u_* \approx U_{10}^n$, was determined. Therefore, the wind-stress coefficient should vary with the wind velocity as $C_{10} \approx U_{10}^{2(n-1)}$. The results, presented in Table 1, indicate that n is always greater than unity, and thus illustrate clearly the increase of stress coefficient with wind velocity in each investigation.

Some of the studies listed in Table 1 were conducted at limited fetch, where the fetch variation of wind-stress coefficient as shown in Fig. 2 is considerable. Such a variation may account partially for the scattering of the results from one set of data to the other. However, the increase of wind-stress coefficient with wind velocity for any one of the studies conducted at a given fetch is well illustrated in Table 1. In any event, the scattering of the results shown in Table 1 indicates that refinements of the coefficient and exponent of the power law shown in Eq. (10) appear to be unwarranted.

2) EARLIER AND PRESENT COMPILATIONS

The earlier compilation (Wu, 1969a) made no distinction between the data collection methods, including wind profile, eddy correlation and surface tilting. In the past decade, we have seen a steady gain of support of the first two methods and a fast erosion of support of the last method; among other deficiencies, the measurement of surface tilt with a surface wave gage was considered (Longuet-Higgins and Stewart, 1964) to be seriously influenced by the wave setup. Consequently, nine sets of data obtained with the surface tilting method in the earlier compilation are excluded from the present analysis. The remaining 21 sets in the previous compilation obtained with the eddy-correlation and wind-profile methods are supplemented by 12 sets of recent results listed in Table 1 obtained with the same techniques.

As in the previous report (Wu, 1969a), the compiled data were also averaged; the process involves first dividing the wind velocity into bands, each band 1 m s^{-1} with its upper and lower bounds at the integral velocities, and then sorting the data into and averaging the sorted data within each band. Since there were significant differences in the number of data points in the various investigations, care had to be taken to avoid the dominance of the averaging by those sets with numerically more data points. Thus the data from each investigation were put through the averaging process first before the final averaging. In other words, if within any band there were more than one data point from any individual investigation, the data were averaged and the averaged data were used in the final averaging.

The final averaged data from 21 sets of earlier results (Wu, 1969a) and 12 sets of recent results are shown in Fig. 4a, and from all 33 investigations in Fig. 4b. The empirical formula [Eq. (10)] suggested earlier (Wu, 1969a) as the simplest form of representing the data for *all* wind velocities, is shown as a dashed line in Fig. 4b. This expression does not approximate the newly averaged results as closely as the linear-law representation

$$C_{10} = (0.8 + 0.065 U_{10}) \times 10^{-3}, \quad U_{10} > 1 \text{ m s}^{-1}. \tag{11}$$

The above expression is shown as a solid line in Fig. 4b and, again, is fitted for the purpose of providing approximations in the simplest forms. It compares very favorably with $C_{10} = (0.75 + 0.067 U_{10}) \times 10^{-3}$ suggested by Garratt (1977).

3) SOME INTERESTING TRENDS

The 21 sets of results compiled earlier (Wu, 1969a) are shown in Fig. 4a to be indistinguishable from the 12 sets of recent data. Furthermore, the empirical formula [Eq. (11)] suggested here is also essentially the same as that proposed by Garratt (1977) averaged from 17 selected sets of results. The latter trend indicates that the averaging of results from various investigations is helpful in avoiding variations due to experimental conditions, techniques and data analysis. The former trend indicates that despite recent refinement of measurement and analysis techniques the same results have been obtained as in earlier investigations. In other words, further measurements of the same type for the same wind velocity range may not be necessary. More studies, however, are needed to uncover other parameters influencing wind-wave interactions such as wind gustiness, swells and currents, which are believed to be the major factors causing the discrepancies in the wind-stress data obtained by various investigators.

In the earlier compilation (Wu, 1969a), the wind-stress coefficient appeared to reach a constant value of 2.6×10^{-3} for $U_{10} > 15$ m s^{-1}. Although there are still slight indications of this trend in the present compilation as well as in Garratt's (1977), the earlier distinct discontinuity appears due to the inclusion of the results obtained with the surface-tilting method, mostly at high wind velocities. There are few sets of data at the high wind velocities ($U_{10} > 20$ m s^{-1}) discussed by Garratt (1977). The quality of these data, understandably, may not be at the same level as those obtained at the lower wind velocities included here. Moreover, as will be discussed later, the general concept of using the roughness length to characterize the sea surface, the basis of present data analysis, may also be questionable under hurricane conditions at very high wind velocities. We choose at this time not to average these data and also to urge more studies at high wind velocities.

b. Boundary-layer characteristics, wind-wave interaction regimes and the Charnock constant

From the averaged data shown in Fig. 4b, we calculated and plotted the roughness Reynolds number, $R_r = u_* z_0/\nu$, in Fig. 5a, in which the critical values of R_r for various boundary-layer regimes (Schlichting, 1968) are also indicated. The roughness Reynolds number is seen in the figure to increase very rapidly with wind velocity for $U_{10} > 2.5$ m s^{-1}. The atmospheric surface layer appears to be aerodynamically smooth ($R_r < 0.17$) for $U_{10} < 3$ m s^{-1}, and aerodynamically rough ($R_r > 2.33$) for $U_{10} > 7.5$ m s^{-1}. The wind friction velocity corresponding to the latter wind velocity is ~26.9 cm s^{-1}.

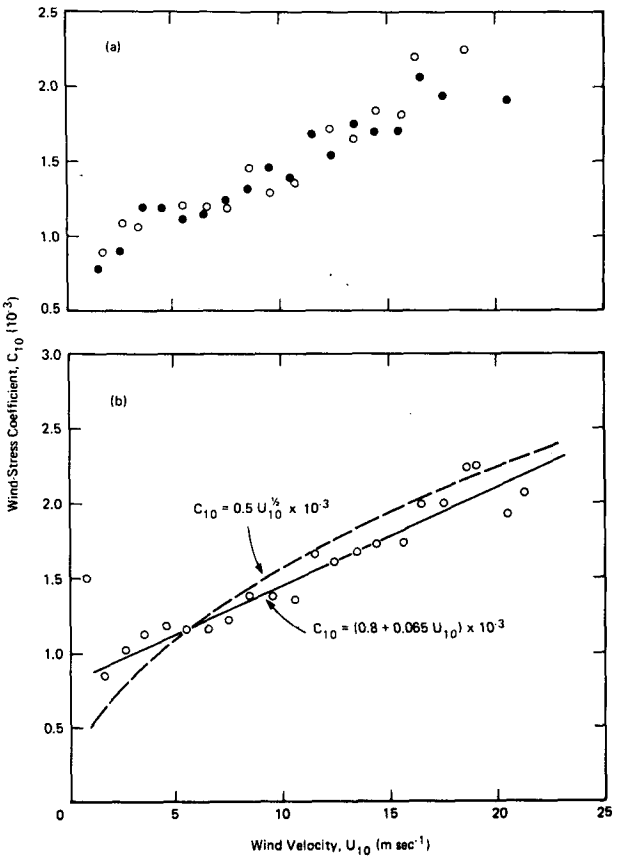

FIG. 4. Variations of wind-stress coefficients with wind velocity. The data averaged from 21 sets of earlier compilation (Wu, 1969a) are shown as open circles in (a) along with those averaged from 12 sets of recent results as solid circles; and the data averaged from all 33 sets are shown in (b).

We can also determine from the Charnock relation the critical friction velocity at which the surface layer becomes aerodynamically rough. This is illustrated by substituting the Charnock relation with $a = 0.0185$ into the expression for the critical roughness Reynolds number:

$$u_* z_0/\nu = 2.33, \quad u_*(0.0185 u_*^2/g)/\nu = 2.33,$$
$$u_* = 26.3 \text{ cm s}^{-1}. \tag{12}$$

Any slight difference in the value of the Charnock constant used here is again not important in the deduction, because the cube root of this value is involved.

The roughness length (z_0) is plotted against the friction velocity in the form of u_*^2/g in Fig. 5b; the data in the aerodynamically rough regime are shown as solid circles and those in the transition region as open circles. In this plot the Charnock constant can be determined directly from a straight line with slope of unity fitted to the data instead of indirectly from the C_{10} vs U_{10} diagram, as is customarily done. A

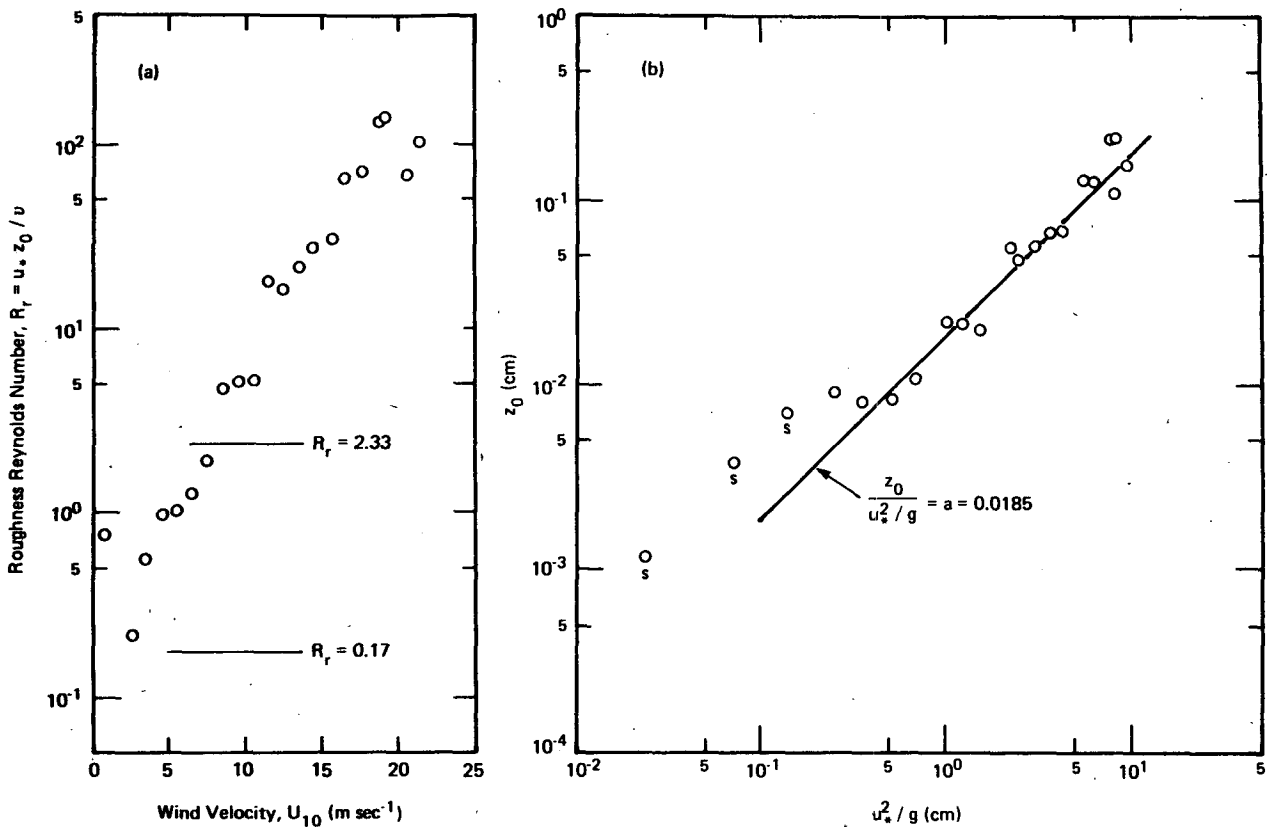

FIG. 5. Boundary-layer regimes and Charnock relationship.

diagram similar to Fig. 5b was used in earlier studies (Wu, 1968, 1969a); however, instead of using logarithmic scales, the data were plotted on linear scales, on which (unlike Fig. 5b) the data at low wind velocities are congested near the origin and more weight was inadvertently assigned to data at high wind velocities. Consequently, a greater value for the Charnock constant ($a = 0.027$) was obtained for the field data (Wu, 1970).

The Charnock relation, shown as a solid line in Fig. 5b, is a good representation of the overall trend of the data for $U_{10} > 5$ m s^{-1}; at lower wind velocities with the data pointed marked with s, the surface layer appears very close to aerodynamically smooth. The Charnock line in the figure can be expressed as

$$z_0 = au_*^2/g, \quad a = 0.0185. \tag{13}$$

It has been shown (Wu, 1970) that the Charnock constant depends on the value adopted for the von Kármán constant. The most recent review by Garratt (1977) provided $a = 0.0144$ for $\kappa = 0.41$, which according to Wu (1970) corresponds to $a = 0.017$ for $\kappa = 0.4$, differing only slightly from our earlier result (0.0156) and the present values.

The close representation of the data in Fig. 5b by the Charnock relation indicates, as proposed earlier (Wu, 1968), that gravitational effects dominate wind-wave interactions. The presentation in Fig. 5b reveals that the data do not conform in very detailed form with the Charnock relation. According to the latter, the roughness length grows with the square of the wind friction velocity, while the data presented in Fig. 5b show a slightly faster rate of growth of roughness length with wind friction velocity. This trend, as discussed in the next section, was apparently concealed in earlier presentations, where the overall correlation rather than the detail trend is emphasized. This trend can be even more easily seen if we take only those data in the aerodynamically rough regime; more will be discussed in a later section.

4. Limitation and refinement of the Charnock relation

a. Intrinsic errors in the Charnock relation and in determining the Charnock constant

The value of the Charnock constant (a) was first estimated from a laboratory study to be 0.012 (Wu, 1968) and from the correlation of laboratory and field data to be 0.0156 (Wu, 1969b). Later, as discussed earlier, the value of a was shown (Wu, 1970) to depend rather strongly on the value taken for the von Kármán constant. Based on compiled oceanic

data alone (Wu, 1969a), it was suggested $a = 0.027$ for $\kappa = 0.4$. On the basis of their compiled data, Kitaigorodskii and Volkov (1965) suggested a different value, 0.035. More recent compilations of oceanic data provide the values of 0.013 (Smith and Banke, 1975) and of 0.0144 (Garrat, 1977) for $\kappa = 0.41$. Although different values of κ and different sets of data were used by various investigators, the discrepancy among the values of a is believed to be primarily due to intrinsic errors in the Charnock relation and in the curve-fitting process used to determine the Charnock constant.

1) Errors related to wind-stress coefficient

The intrinsic error in the Charnock constant results from the definition of the roughness length, a sensitive function of the stress coefficient, and from inevitable error in determining the stress coefficient. Using Eq. (3) these errors can be expressed as

$$\left.\begin{aligned} \frac{da}{dC_{10}} &= \frac{gZ}{{U_{10}}^2}\left[\frac{\kappa/(2{C_{10}}^{1/2}) - 1}{{C_{10}}^2 \exp(\kappa/{C_{10}}^{1/2})}\right] \\ \frac{\Delta a}{a} &= \frac{C_{10}}{a}\frac{\Delta C_{10}}{C_{10}}\frac{da}{dC_{10}} \end{aligned}\right\}, \qquad (14)$$

where Δa and ΔC_{10} are the probable errors in determining a and C_{10}, respectively. If we substitute Eq. (10) into Eq. (14), we have $da/dC_{10} = 100$, 68 and 46 at $U_{10} = 5$, 10 and 15 m s^{-1}, respectively. The probable error of field measurements of C_{10} was considered to be no less than 10%, or $\Delta C_{10}/C_{10} \approx 0.1$. Therefore, if we take $C_{10}/a \approx 0.1$, a variation of a in the order of 55–70%, as shown in the previous paragraph, is expected; this variation doubles if the error in determining C_{10} reaches 20%.

2) Errors related to curve fitting

As discussed previously, the Charnock constant can be determined by fitting a straight line with a slope of unity to the data presented in Fig. 5b. An earlier compilation (Wu, 1969a) including the data determined with the surface-tilting method shows a much faster rate of increase of z_0 with ${u_*}^2/g$; this is also true for portions of the data compiled by Garratt (1977), as discussed in the next section. In this case, if more weight is assigned to data at low wind velocities, such as in the case where data at high wind velocities are not available, a smaller value of Charnock constant is obtained. If more weight is assigned to data at high wind velocities, such as in the case discussed previously where data are plotted on linear scales, a greater value of the Charnock constant is obtained. These trends can be easily seen in Fig. 5b. However, as pointed out earlier, this is the first time the data have been presented in this form, which also reveals other weakness of the Charnock relation mentioned earlier and to be discussed in the next section.

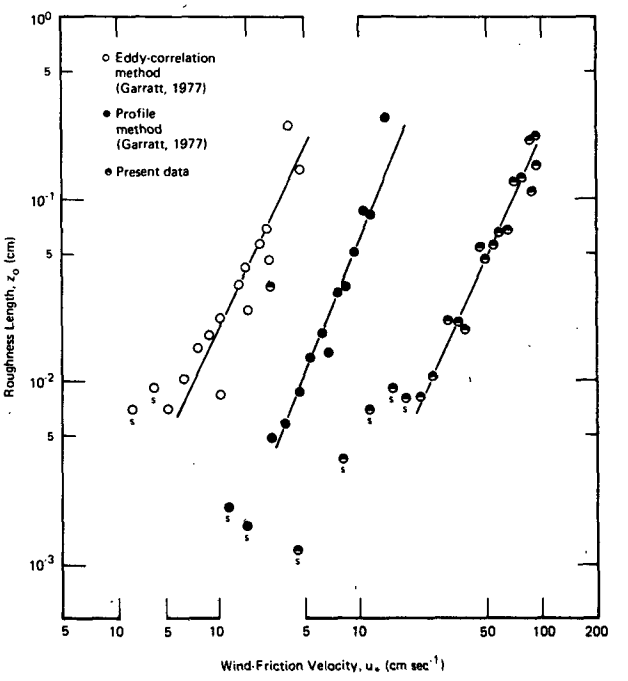

FIG. 6. Variation of roughness length with wind friction velocity. The data points marked with s are from the aerodynamically smooth flow regime.

In summary, with the errors discussed above, it is not really surprising that different values of the Charnock constant are determined from different investigations.

b. *Refinement of the Charnock relation*

The roughness lengths and friction velocities calculated from the averaged data reported by Garratt (1977) and from the present data shown in Fig. 4b are presented in Fig. 6. There are two sets of averaged data presented by Garratt, one set of stress coefficients using the wind-profile method and the other set with the eddy-correlation method; the present data make no distinction between the methods. A straight line is then fitted to each set of data, except those in the aerodynamically smooth regime ($z_0 u_*/\nu < 0.17$) indicated by s in the figure. One data point at the highest wind friction velocity of the wind-profile method compiled by Garratt, obviously deviating from the otherwise consistent trend, is also omitted from the curve fitting. The slopes of the straight lines shown in Fig. 6 are presented in Table 2.

According to the Charnock relation, the roughness length varies with the square of the wind fric-

TABLE 2. Values of exponent β in $z_0 \approx u_*^{\beta}$.

Data source	Garratt (1977) Eddy-correlation method	Garratt (1977) Wind-profile method	Present data (Fig. 4b)
β	2.25	2.45	2.25

tion velocity. All three sets of data in Fig. 6, however, indicate clearly that roughness length increases with wind friction velocity more rapidly than this rate. It has long been suggested that the equilibrium state of wind-wave interaction should be influenced to some extent by both surface tension and viscosity. Including these two parameters, the following can be grouped on the dimensional grounds:

$$z_0 = \frac{au_*^2}{g}\left(\frac{\mu u_*}{\sigma}\right)^{\beta-2}, \quad 2 < \beta < 2.5, \qquad (15)$$

where μ is the viscosity of water, σ the surface tension, and the values of β are shown in Table 2.

The effects of surface tension and viscosity appear to be negligible at high wind velocities in laboratory tanks (Wu, 1968). In this case, the roughness elements consist of dominant waves, from which airflow separates. The influence of surface tension is absent as these dominant waves are gravity waves, and the influence of viscosity is insignificant as the viscous dissipation of these "long" waves is very gradual. The situation, however, is very much different in the field, where the wave crests from which airflow separates are very far apart. Between separation pockets the airflow is retarded by resistance provided by much shorter waves, of which the propagation is undoubtedly affected by surface tension and of which the viscous damping is considerable.

More studies, especially those under controlled conditions, are needed to establish the functional relationship suggested in Eq. (15). A value of β lying between 2 and 2.5 indicates that gravity is still seen as the most important parameter governing wind-wave interaction; dynamically, the relative contribution of gravitational acceleration is proportional to u_*^2. Surface tension and viscosity are less important parameters but are definitely not negligible; dynamically, the combined relative contribution of these two parameters is proportional to $u_*^{\beta-2}$, where β-2 as shown in Table 2 very likely has a value of about ⅓.

5. Discussion

a. Roughness elements and dominant waves

Using the data compiled earlier (Wu, 1969a), the ratios between the dominant wave height $H_{1/3}$ and the physical roughness length k for both laboratory and oceanic conditions were calculated by Wu (1972) and are reproduced in Fig. 7. The height of dominant waves is seen to be comparable with the height of roughness elements at high wind velocities in laboratory tanks, and is seen to be much greater than the height of roughness elements in the ocean. The choice of anemometer height and any slight differences in wind-stress data are not crucial for the present order-of-magnitude comparison. It is clear, as illustrated by the inserts in Fig. 7, that the airflow separates from dominant waves in tanks and separates from short waves superimposed on the dominant waves in the ocean.

One of the basic problems in connection with wind-wave interaction has been to determine the portion of the wave spectrum supporting the bulk of the wind stress. The importance of short waves in transferring momentum from wind to waves was suggested earlier by a number of investigators (e.g., see Munk, 1955). More recently, as discussed above, the role played by short waves as roughness elements has been more clearly established, and the length of these short waves can also be identified (Wu, 1970) as seven times the roughness height k_g shown in Fig. 3. The concept that long waves themselves do not act as roughness elements but modify the roughness density has been illustrated through measurements of the wind boundary layer in a wind-wave tank with and without preexisting long, regular surface waves (Wu, 1977). The presence of long waves was found to reduce the density of roughness elements. Consequently, despite the height of dominant waves with the presence of preexisting waves being about three times greater than that without the presence of preexisting waves, the roughness length is reduced at low wind velocities and remains the same at high wind velocities.

Some interesting results on the frequencies of occurrence of sea surface irregularities were reported by Kondo *et al.* (1973); these irregularities are ocean waves of high frequencies 10–220 rad s^{-1}. They then suggested that the most frequently occurring height of irregularities (h_p) was similar to the roughness length. The representative heights which they determined are plotted as a function of the roughness lengths calculated from $30(au_*^2/g)$ in Fig. 8, where $a = 0.0156$, as their experiments were performed at a relatively short fetch. Actually, the value of the Charnock constant is not particularly important; if the irregularity and the roughness length are indeed similar, we should be able to fit the results presented in Fig. 8 with a straight line having a slope of unity. However, as indicated in the figure, the data follow two broken lines with much smaller slopes. It appears that the two quantities are roughly comparable at the joint of two

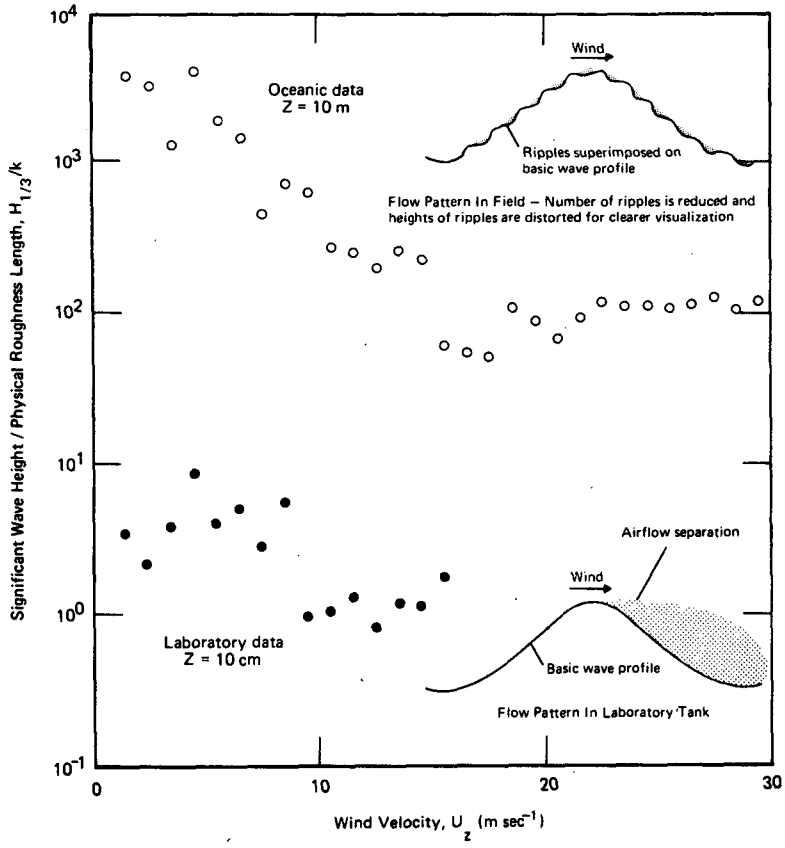

FIG. 7. Comparisons between significant wave height and roughness height and illustrations of different airflow patterns in laboratory tanks and in the field.

broken lines corresponding to approximately $U_{10} = 6.5$ m s^{-1}. Toward lower wind velocities, the irregularity determined by Kondo *et al.* overrepresents the roughness length, and toward the higher wind velocities the irregularity underrepresents the roughness length. Nonetheless, their effort is certainly worthwhile and should be further pursued.

An expression primarily for determining the roughness length in the field was suggested by Hsu (1974): $z_0 = (1/2\pi)H_d/(c_d/u_*)^2$, where H_d and c_d are the height and the phase velocity of dominant waves, respectively. His expression can be rearranged into a simpler and clearer form as $z_0/(u_*^2/g) = H_d/\lambda_d$, where λ_d is the length of dominant waves. In other words, the Charnock constant is suggested in this form to be the same as the steepness of the dominant waves. Drastically different airflow patterns in laboratory tanks and in the field over roughness elements and dominant waves are illustrated in Fig. 7. Nonetheless, a combination of both laboratory and field results on roughness lengths was used by Hsu to substantiate his argument. In any event, such a correlation relating roughness length and wind friction velocity to dominant waves in the field lacks a physical basis. The dominant oceanic waves, of which phase velocity is about the same as wind velocity, simply do not act as roughness elements supporting wind stress. The main point suggested by Hsu is that the Charnock constant varies and approaches a constant value only when the sea state develops toward saturation. However, most, if not all, of the results cited by him were obtained under a "saturated" state.

b. Wind-stress coefficient and roughness Reynolds number

Over a solid rough surface, as velocity increases, the viscous sublayer becomes thinner and the roughness elements start to protrude through the sublayer. Subsequently, any further increase of velocity causes more protrusion of the elements, of which form drag shares a greater portion of the shear stress applied by the flow on the boundary. In the meantime, following more protrusion of roughness elements, the roughness length, a statistical description of density and height of the elements, increases. Eventually, the sublayer is totally disrupted with the

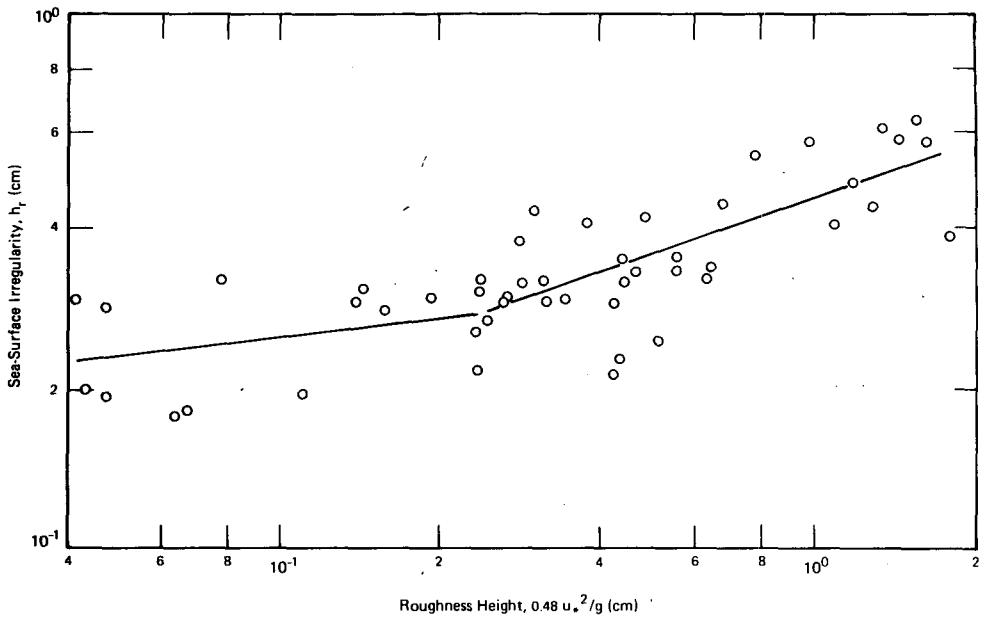

FIG. 8. Sea surface irregularities (Kondo *et al.* 1972) and roughness lengths.

roughness elements being fully exposed at even higher velocities; the form drag of the elements then supports the total shear stress. This is the fully rough condition, where the roughness length no longer varies with increasing velocity and the stress coefficient therefore has a constant value. The entire sequence of development can be described by the roughness Reynolds number $u_* z_0/\nu$.

Over the air-sea interface, short waves are the roughness elements. Many of the physical arguments applied over solid surface still hold here, except that the roughness elements at the interface grow with wind velocity even in the fully rough regime. Consequently, the wind-stress coefficient increases continuously with wind velocity, as shown in previous sections. It is exactly for this reason that we have a wind-wave interaction problem. Physically, the correlation between the wind-stress coefficient and the roughness Reynolds number reported by SethuRaman and Raynor (1975) is fully expected, since a functional relationship between them can be derived from the logarithmic wind profile and the definition of stress coefficient as discussed earlier as well as by Leavitt (1976). Experimentally, large errors in measurements of the wind stress could be hidden in this type of C_{10} vs R_r presentation. Practically, relating the wind-stress coefficient to the roughness Reynolds number (SethuRaman and Raynor, 1975) by a series of empirical formulas for various flow regimes has no use. For applications, the wind-stress coefficients must be related to the wind velocity and fetch, not to the roughness Reynolds number, which itself must be determined from the wind-stress coefficient.

c. Wind-stress coefficients and wind velocity

As discussed previously, the wind-stress coefficient must increase with wind velocity if the wind velocity follows a logarithmic profile and the Charnock relation holds. Failing to recognize this, some investigators have accepted the logarithmic profile and the Charnock relation on one hand, and suggested a constant wind-stress coefficient on the other. Furthermore, as also pointed out by Garratt (1977), in some cases, despite results which illustrate only an approximate increase of the wind-stress coefficient with wind velocity, a mean line was drawn through the data to represent a constant coefficient. This is done on the basis of a rationale that the wind-stress coefficient should be considered as constant if there is no well-established trend indicated by the data. Recently, with the refinement of measurements and the demand for a more accurate estimation of the wind stress, the view of the wind-stress coefficient increasing with wind velocity has slowly gathered more support (Smith and Banke, 1975).

Over the most frequently occurring wind velocity range ($1 \text{ m s}^{-1} < U_{10} < 20 \text{ m s}^{-1}$), the wind-stress coefficient is seen in Fig. 4 to increase with wind velocity. In any event, the rationale ought to be that the wind-stress coefficient should be considered to increase with wind velocity unless there is overwhelming evidence indicating a constant stress coefficient. The basis for advancing such a rationale is simply that the stress coefficient is directly related to the roughness length, which grows with wind velocity, as discussed in detail in the preceding section. A relatively large wind-stress coefficient

is shown at $U_{10} = 0.5$ m s^{-1}; this is also substantiated by the friction coefficient over a solid surface in an aerodynamically smooth flow, where the friction coefficient decreases with increasing velocity (Schlichting, 1968). At high wind velocities ($U_{10} > 20$ m s^{-1}), a constant wind-stress coefficient again prevails. The sea surface is disrupted at high wind velocities with intensive sea spray. Under these storm conditions, the entire concept of applying the roughness length to the disintegrated air-sea interface may be questionable. Intensive sea spray occurring under these conditions should play a major role in the air-sea momentum transfer, although it is still questionable at how high a wind velocity this would occur. The influence of spray is also not in contradiction with the similarity, pointed out by Garratt (1977), between the wind-stress data obtained in wind flumes and in the field under high wind velocities (hurricanes). At lower velocities with drastically different roughnesses and dominant wave relationships, the flume-determined stress coefficient is much greater than the field-determined value; the similarity at higher wind velocities may result from similar intensive spray.

6. Concluding remarks

The Charnock relation has been fully explored to derive the dependence of the stress coefficient with wind velocity and fetch, and to demonstrate its correlation with the criteria determining airflow separation from waves and boundary-layer regimes of the atmospheric surface layer. On the other hand, the intrinsic error and limitation of this relation are also exposed. As our understanding of wind-wave interaction advances, a more refined parameter describing the equilibrium state between the wind and waves is needed. One possible grouping of three dynamic parameters—gravitational acceleration, surface tension and viscosity—is suggested for further investigations.

For oceanic applications, the wind-stress coefficients reported earlier and those obtained recently are very consistent. The difference between results obtained in individual investigations appears to be due to either the variation of their experimental program including measurement and analysis techniques, or to the omission of some other parameters such as wind gustiness, swells and currents. Further measurements relating wind-stress coefficient to the wind velocity appear to reach the point of diminishing return; to explore these new parameters, on the other hand, should be actively pursued. In addition, the data are very scarce at higher wind velocities (hurricanes). It remains to be seen whether the disintegrated air-sea interface with intensive wave breaking and spray can still be described by the roughness length.

Acknowledgments. I am grateful to Dr. S. D. Smith for his careful review and valuable suggestions which led to substantial improvement of this manuscript. I am also very grateful to the sponsorship of my work by the Physical Oceanography Program, National Science Foundation under Grant OCE 77-26508, and by the Fluid Dynamics Program, Office of Naval Research, under Contract N00014-75-C-0285.

REFERENCES

Banner, M. L., and W. K. Melville, 1976: On the separation of airflow over water waves. *J. Fluid Mech.*, **77**, 825–842.

Brocks, K., and L. Krugermeyer, 1970: The hydrodynamic roughness of the sea surface. Berichte des Instituts für Radiometeorologie und Maritime Meteorologie, No. 14, University of Hamburg.

Charnock, H., 1955: Wind stress on a water surface. *Quart. J. Roy. Meteor. Soc.*, **81**, 639–640.

De Leonibus, P. S., 1971: Momentum flux and wave spectra observations from an ocean tower. *J. Geophys. Res.*, **76**, 6506–6527.

Denman, K. K., and M. Miyake, 1973: The behavior of the mean wind, the drag coefficient and the wave field in the open ocean. *J. Geophys. Res.*, **78**, 1917–1931.

Favre, A., and K. Hasselmann, 1978: *Turbulent Fluxes through the Sea Surface, Wave Dynamics and Prediction.* Plenum Press, 679 pp.

Garratt, J. R., 1977: Review of drag coefficients over oceans and continents. *Mon. Wea. Rev.*, **105**, 915–929.

Gent, P. R., and P. A. Taylor, 1977: A note on "separation" over short wind waves. *Bound.-Layer Meteor.*, **11**, 65–87.

Hicks, B. B., 1972: Some evaluations of drag and bulk transfer coefficients over water bodies of different sizes. *Bound.-Layer Meteor.*, **3**, 201–213.

——, and A. J. Dyer, 1970: Measurements of eddy-fluxes over the sea from an off-shore oil rig. *Quart. J. Roy. Meteor. Soc.*, **96**, 523–528.

Hsu, S. A., 1974: A dynamic roughness equation and its application to wind stress determination at the air-sea interface. *J. Phys. Oceanogr.*, **4**, 116–120.

Kitaigorodskii, S. A., and Yu A. Volkov, 1965: On the roughness parameter of the sea surface and the calculation of momentum flux in the near-water layer of the atmosphere. *Izv. Atmos. Oceanic Phys.*, **9**, 973–988.

Kondo, J., Y. Fujinawa and G. Naito, 1972: Wave-induced wind fluctuation over the sea. *J. Fluid Mech.*, **51**, 751–771.

——, Y. Fujinawa and G. Naito, 1973: High-frequency components of ocean waves and their relation to the aerodynamic roughness. *J. Phys. Oceanogr.*, **3**, 197–202.

Leavitt, E., 1976: Comments on "Surface drag coefficient dependence on the aerodynamic roughness of the sea" by S. SethuRaman and G. S. Raynor. *J. Geophys. Res.*, **81**, 4995.

Longuet-Higgins, M. S., and R. W. Stewart, 1964: Radiation stress in water waves; a physical discussion with application. *Deep-Sea Res.*, **11**, 529–562.

Melville, W. K., 1977: Wind stress and surface roughness over breaking waves. *J. Phys. Oceanogr.*, **7**, 702–710.

Miyake, M., M. Donelan, G. McBean, C. Paulson, F. Badgley and E. Leavitt, 1970: Comparison of turbulent fluxes over water determined by profile and eddy correlation techniques. *Quart. J. Roy. Meteor. Soc.*, **96**, 132–137.

Munk, W. H., 1955: Wind stress on water, an hypothesis. *Quart. J. Roy. Meteor. Soc.*, **81**, 320–332.

Pond, S., G. T. Phelps, J. S. Paquin, G. McBean and R. W. Stewart, 1971: Measurement of turbulent fluxes of momentum, moisture and sensible heat over the ocean. *J. Atmos. Sci.*, **28**, 901–917.

Roll, H. U., 1965: *Physics of the Marine Atmosphere*. Academic Press, 426 pp.

Schlichting, H., 1968: *Boundary-Layer Theory*. McGraw-Hill, 748 pp.

SethuRaman, S., and G. S. Raynor, 1975: Surface drag coefficient dependence on the aerodynamic roughness of the sea. *J. Geophys. Res.*, **80**, 4983–4988.

Sheppard, P. A., D. T. Tribble and J. R. Garratt, 1972: Studies of turbulence in the surface layer over water (Lough Neagh), Part I, Instrumentation, programme, profile. *Quart. J. Roy. Meteor. Soc.*, **98**, 627–641.

Smith, S. D., 1974: Eddy flux measurements over Lake Ontario. *Bound.-Layer Meteor.*, **6**, 235–255.

——, and E. G. Banke, 1975: Variation of the sea-surface drag coefficient with wind speed. *Quart. J. Roy. Meteor. Soc.*, **101**, 665–673.

Wieringa, J., 1974: Comparison of three methods for determining strong wind stress over Lake Flevo. *Bound.-Layer. Meteor.*, **7**, 3–19.

Wu, Jin, 1968: Laboratory studies of wind-wave interaction. *J. Fluid Mech.*, **34**, 91–112.

——, 1969a: Wind stress and surface roughness at air-sea interface. *J. Geophys. Res.*, **74**, 444–455.

——, 1969b: Froude number scaling of wind-stress coefficients. *J. Atmos. Sci.*, **26**, 408–413.

——, 1969c: A criterion for determining airflow separation from wind waves. *Tellus*, **21**, 707–714.

——, 1970: Wind-wave interactions. *Phys. Fluids*, **13**, 1926–1930.

——, 1971: Anemometer height in Froude scaling of wind stress. *J. Waterways Harbors Coastal Eng. Div., ASCE*, **97**, 131–137.

——, 1972: Physical and dynamical scales for generation of wind waves. *J. Waterways Harbors Coastal Eng. Div., ASCE*, **98**, 163–175.

——, 1975: Wind-induced drift currents. *J. Fluid Mech.*, **68**, 49–70.

——, 1977: Effects of long waves on wind boundary layer and on ripple slope statistics. *J. Geophys. Res.*, **82**, 1359–1362.